Reliability of Wind Turbine Power Modules using High-Resolution Wind Data Reconstruction: A Digital Twin Concept

Nikolaos Iosifidis
School of Engineering
University of Warwick
Coventry, UK
Nikos.Iosifidis@warwick.ac.uk

Yanghao Zhong
School of Engineering
University of Warwick
Coventry, UK
Yanghao.Zhong@warwick.ac.uk

Borong Hu
Department of Engineering
University of Cambridge
Cambridge, UK
Bhu529@cam.ac.uk

Biyun Chen
School of Electrical Engineering
Guangxi University
Nanning, China
Chenbiyu@gxu.edu.cn

Li Ran
School of Engineering
University of Warwick
Coventry, UK
L.Ran@warwick.ac.uk

Subhash Lakshminarayana
School of Engineering
University of Warwick
Coventry, UK
Subhash.Lakshminarayana@warwick.ac.uk

Chunjiang Jia
Offshore Renewable Energy Catapult
Blyth, UK
Chunjiang.Jia@ore.catapult.org.uk

Paul McKeever
Offshore Renewable Energy Catapult
Blyth, UK
Paul.McKeever@ore.catapult.org.uk

Chong Ng
Offshore Renewable Energy Catapult
Blyth, UK
Chong.Ng@ore.catapult.org.uk

***Abstract*— This study introduces a Digital Twin (DT) framework for the reliability assessment of wind turbine power modules. Its importance is demonstrated by examining the effect of wind turbulence on the electrothermal behaviour and lifetime of machine side power electronic converters and semiconductor devices of direct-drive wind turbines. To this end, an electrothermal model embedded in a turbine model is established, which tracks the changes in wind speed. Using real-world, 1-sec wind speed data, the real device junction temperature profiles and the fatigue experienced by the semiconductor devices are examined for two 10-min periods. Then, these metrics are compared with the corresponding metrics of the same 10-min periods when the wind speed is assumed constant and equal to the 10-min average value, which is often used in traditional device reliability assessment methods using SCADA data. Based on simulation results, the fatigue experienced by the semiconductor devices due to sudden fluctuations of the wind is found to be significantly higher than the fatigue estimated by traditional reliability assessment methods using the SCADA data. Two methods that attempt to reconstruct the wind spectrum (Random Walk Metropolis-Hastings algorithm) and compress the wind speed data (Discrete Wavelet Transform) are proposed. These and/or other similar methods may be integrated into the DT interface to address the issue of the large volume of data required to be stored in DTs.**

Keywords—Digital Twin, Data compression, Wind turbulence Reliability assessment, Power Electronic Converters

I. INTRODUCTION

Surveys on onshore wind turbines (WT),[1][2], quantify the failure rates and downtimes of WT components. The findings show that power converters have considerably high failure rates, but low downtimes. However, the downtimes will inevitably increase for offshore WTs due to the remoteness of the sites and the harsh weather conditions that often make the on-site maintenance not feasible. Furthermore, the failure rates also increase for larger WTs [2], which is often the case in offshore sites. A review on power electronic converters states that 34% of the failures occur on the semiconductors and the solder [3]. Additionally, the study connects the predominant failure mechanisms, bond wire lift-off and solder fatigue, to localized device temperature swings due to device heating.

This study focuses on the direct-drive (DD), variable speed, offshore WT power conversion systems. These systems incorporate fully rated power converters to facilitate the variable speed operation between a specified cut-in and a rated cut-off wind speed. As a result, the condition and lifetime of the power converters are subject to stochastic aerodynamical loads. In design modification and condition-based maintenance, the condition and lifetime of the power electronic devices are assessed by using historical operational data by the means of simulation models and methods for fatigue estimation [3]. The degradation of the devices can be predicted beforehand, and thus the costs of maintenance can be reduced. Traditionally, in these studies, the operational data are gathered from SCADA measurements, with a sampling frequency of 10 minutes for long-term storage. For example, SCADA stores the average, maximum, minimum, and standard deviation of the wind speed every 10 minutes. However, early work in wind spectra suggests high turbulence of the wind in the timescales spanning from a few seconds to 10 minutes, with a distinct peak at 1 minute [4]. The 10-min average wind data cannot capture the dynamic character of the wind, i.e. turbulence, which consists of frequent and unpredictable fluctuations in the short timescale, lasting tens of seconds [5]. These fluctuations affect the electrothermal behaviour of the power devices, often causing thermal cycling on the fully rated power converters, resulting in increased degradation. Such effects could be lost in the 10-min average value granularity which is currently used to estimate the lifetime. Thus, methods that can capture the turbulence features of the wind more accurately are necessary to improve the condition monitoring (CM) task and enhance the credibility of the reliability assessments.

To overcome these drawbacks, we propose a digital twin

(DT) framework for the reliability assessment of power electronic devices in WTs. We analyze the advantages of DTs over the traditional methods by using an electrothermal model to simulate the electrothermal behaviour of the power modules using real-world high-frequency sampled wind data (at 1-sec intervals). To assess the condition of the semiconductor devices, we use material fatigue estimation methods. We present a comparison between the results from 10-min average wind speed data and 1-sec wind speed data, which highlights the advantages of DTs for CM tasks. Finally, we suggest two methods for the task of wind data compression and wind spectrum reconstruction.

II. Digital Twins

A. *Introduction to Digital Twins*

The initial definition of a DT, given by Grieves [6], defines the DT concept as a three dimensional (3-D) entity consisting of 1) a physical product in real space, 2) a virtual product in the virtual space, 3) the interconnection of data and information between the two. In the virtual space, the virtual product is a replica of the physical product, experiencing the same conditions (operating, environmental, etc.) as the real product and evolving identically through time.

With advancements in network architecture, cyber physical systems (CPS), Internet of Things (IoT), artificial intelligence (AI), machine learning (ML) and data science, DTs are finding more and more industrial applications. As the applications of the DTs become more complex, the concept of DT is becoming more sophisticated. Tao et.al. proposed a 5-D DT, adding the DT data and DT services to the original 3-D DT [7]. For instance, the data gathered from the physical equipment can be transferred to the virtual space using IoT to be stored and analysed online, in cloud platforms. Subsequently, by using methods of data science, ML, and AI, the data can be transformed into meaningful information which describe the physical system. In order to achieve optimal results, the 5-D DT proposes a fusion of data which integrates information from both the physical space (operational data, environmental factors, etc.) and the virtual space (simulation results, predicted values and states).

DT services consist of predefined functions and models which utilize the DT's data to obtain information on the system's condition and performance. Furthermore, DT services assist the system operator to interact with the DT environment. For example, when the DT is tuned to monitor the electrothermal behaviour of the power conversion system, lifetime, reliability, and fault detection models can be embedded in the DT interface. Thus, the operator of the DT can acquire important information on the condition of the system such as the fatigue experienced by the devices and their state of health, at any given time. DT services may also be used to analyze fault indicators (e.g., abnormally high temperatures, currents, etc.), predicting how the system will evolve based on these indicators. ML algorithms and pre-trained neural networks (NN) may be used for that task. In [8], the authors review ML methods used for CM of various WT components. Based on the fused DT data and the DT services, the information from the physical products and virtual models are transformed into meaningful and actionable information that the operator can act upon, depending on factors such as fault indictors and their significance, damage accumulation and state of health of the power devices.

B. *Digital Twin for reliability assessment of wind turbine power modules*

A case study on 5-D DT on a WT was conducted in [9], to identify abrupt failures in the WT gearbox. The principles and methodology of [9] may be extended for the present case. The proposed workflow of the 5-D DT for reliability assessment of power modules is illustrated in Fig.1.

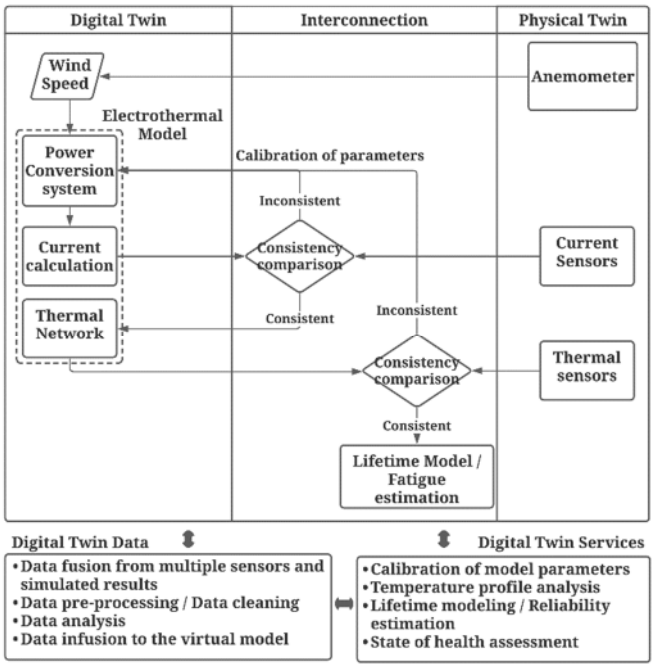

Fig. 1. Workflow of the DT for reliability assessment of power modules.

In the proposed framework, wind speed measurements from the on-site sensors (anemometers) are fed into the virtual electrothermal model of a WT drivetrain. The simulated current and temperatures of the devices are compared with the real measurements from on-site sensors to assess whether the DT is tuned. In the case of a fine-tuned DT, utilizing the embedded lifetime and reliability models within the DT services, the damage accumulated on the semiconductors and the state of health of the power module can be assessed. If the parameter difference between the physical converter and the virtual model exceeds a specified error limit, some actions are required to pinpoint which system is the one at fault. The method suggested for that task in [9], compares the real measurement and the simulated results against a reference state. In case only the simulated results deviate from the reference state, the virtual model requires tuning, and the model parameters are calibrated. In case only the physical measurements deviate from the reference state, an abrupt failure has probably occurred on the power converter, which the virtual model is unaware of. Subsequently, some actions must be implemented on the system by the DT operator to control the device remotely. Furthermore, the simulation model's parameters will require calibration to be updated to the model's new state. Finally, if the parameters of both the physical converter and virtual model deviate from the reference state, the virtual model parameters need to be calibrated first. Model parameter calibration may be achieved with regression and other optimization methods. For instance, in [10], the authors used Particle Swarm Optimization (PSO) to adjust the simulation model internal parameters of a DC-DC power converter.

Failure prognosis based on several health indicators, abrupt failure diagnosis, and device state of health assessment are some of the DT features that may be implemented for WT power modules. However, these are not the main focus of this study. In the present work, the wind turbulence effect on the electrothermal behaviour and the lifetime of the fully rated converters is investigated. Comparing high-frequency sampled wind speeds with 10-min average wind speeds that are currently used for reliability analysis, the advantages of the DT concept for reliability assessment of the power electronic devices are highlighted. Furthermore, the following analysis aims to fill a gap in literature that has not yet quantified the effect of the wind turbulence on the lifetime of semiconductor devices due to temperature fluctuations occurring within tens of seconds.

III. Wind Data Compression And Reconstruction

One of the issues that DTs face is the large volume of data required to be transferred and stored. As the WTs have multiple sensors in all their subcomponents, the costs of data storage of high-frequency sampled data might be very high and cost-wise unjustifiable. Therefore, methods that compress the wind data and reconstruct the wind spectrum are worth exploring.

A. Random Walk Metropolis-Hastings algorithm

A Markov Chain Monte Carlo (MCMC) method named Random Walk Metropolis-Hastings (RWMH) algorithm is proposed for the task of wind spectrum reconstruction. An advantage of this method is that it requires very little information that is already present in the current 10-min SCADA measurements, i.e., the average wind speed, and its standard deviation of every 10 minutes. The algorithm samples randomly from a proposed distribution and applies an accept/reject feature to build the time-series. Bibliography and early work in the wind spectra suggests that the wind speed follows a Gaussian distribution in the 10-min timeframe [11]. Therefore, the RWMH algorithm samples from Gaussian distributions, making the MCMC algorithm faster as the distribution is symmetric. A disadvantage of the RWMH is the fact that it builds the wind spectrum randomly, and it does not resemble how the real wind spectrum evolved during these 10 minutes. However, all the turbulence features of the wind are captured by this method, and thus, the wind turbulence effect on the lifetime of power modules can be described. Further details can be found in [12] [13], and the algorithm is summarized below:

Random Walk Metropolis-Hastings algorithm

Step 1. Sample a random point, θ^0, from a Gaussian distribution, $q(\theta)$, with mean and standard deviation corresponding to a SCADA measurement.

Step 2. Start the iterative process. For each iteration, $i = 2, \dots N$, follow the steps:

a. Sample a candidate random sample, θ^{cand}, from the proposal Gaussian distribution, $q(\theta)$, with mean equal to the previous point, θ^{i-1}, while the variance remains unchanged. Centering the candidate sample to the previous iteration makes the process a random walk.

$$\theta^{cand} \sim q\left(\theta^i \middle| \theta^{(i-1)}\right) \tag{1}$$

b. Calculate the acceptance probability of the candidate sample, α, which for symmetric distributions is:

$$\alpha\left(\theta^{cand}, \theta^{(i-1)}\right) = \frac{p(\theta^{cand})}{p(\theta^{(i-1)})} \tag{2}$$

where $p(\theta)$ is the probability density function of the Gaussian distribution.

Step 3. Accept or reject the candidate sample, θ^{cand}, according to the following criteria:

a. If $\alpha\left(\theta^{cand}, \theta^{(i-1)}\right) \geq 1$, always accept the candidate sample.

b. If $\alpha\left(\theta^{cand}, \theta^{(i-1)}\right) < 1$, then the sample can be accepted or rejected based on:

i. Generate a uniform random variable between 0 and 1, $u \sim U(0,1)$.

$$\theta^i = \begin{cases} \theta^{cand}, & if\ u \leq a \\ \theta^{(i-1)}, & if\ u > a \end{cases} \tag{3}$$

Step 2 implies an autocorrelation factor between consecutive wind speeds, resembling the realistic wind spectra. The accept/reject feature of Step 3 emulates the sudden and unpredictable fluctuations of the wind in the short timescales. To validate the RWMH algorithm as a method to reconstruct the wind spectrum, two sample paths are generated and compared with the real wind speeds in Fig 2; one near the cut-in wind speed (4m/s) and one near the nominal wind speed (12m/s). The metrics of the RWMH algorithm resemble the real ones, even though they are randomly sampled, implying a good accuracy of the method.

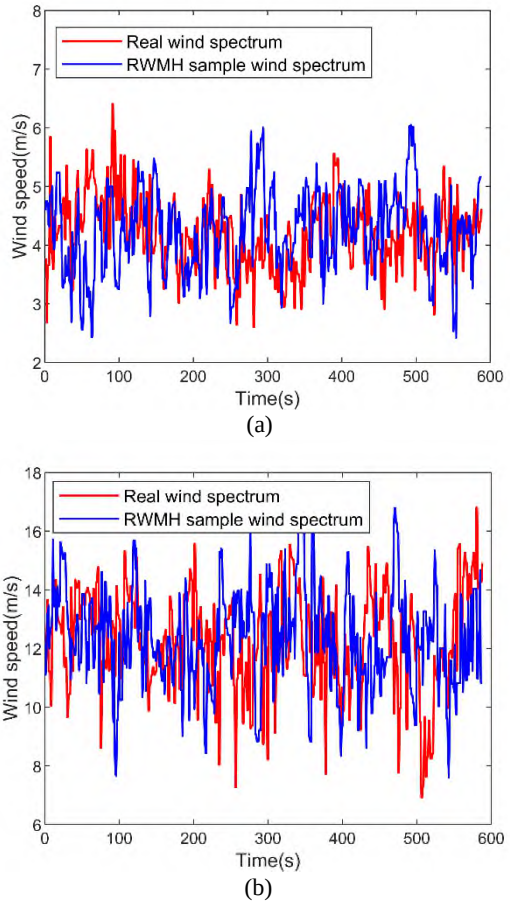

Fig. 2. Comparison of the RWMH generated wind spectrum with the real wind spectrum for (a) low winds, (b) medium winds.

Despite the favourable results, as noted above, the RWMH method builds the wind spectrum randomly, and hence, the match between the reconstructed wind spectrum and the actual one is random as well. To overcome this issue, in the following, we propose a deterministic method that compresses/reconstructs the wind speed data using the Wavelet Transform (WTr).

B. Wavelet Transform method

To address the issue of the large volume of data that are required to be stored, several methods of data compression may be implemented by the DT services. Wavelet Transform (WTr) is a powerful tool for the analysis and compression of time-limited and non-stationary signals such as the wind speed data. WTr is similar to the well-known Fourier Transform (FT). However, it overcomes a key drawback of FT, in that, although FT provides a very precise analysis of the frequencies contained in the signal, it does not give any indication of when those frequencies occur. On the other hand, WTr is a multi-resolution transform, which allows for time-frequency analysis, i.e., the information about when certain features occur in the signal can be obtained. It is very useful for compression since changes at finer scales can be omitted during the compression stage. WTr accomplishes this by convolving the time-series signal with a series of basis functions called the "wavelet family", which in turn consists of a series of time-shifted and scaled versions of the so-called "mother wavelet". Examples of mother wavelets include the Haar wavelet, Daubechies wavelet, Fejer-Korovkin wavelet, and Biorthogonal wavelet, amongst others [14]. Mathematically, a mother wavelet signal can be represented by:

$$\varphi_{(a,b)}(t) = \frac{1}{\sqrt{a}}\varphi\left(\frac{t-b}{a}\right) \quad (4)$$

where b is the shift factor and a is the scaling factor that compresses or dilates the wavelet. Then, the WTr of a time signal f(t) is given by:

$$W\,f(a,b) = \int_{-\infty}^{\infty} f(t)\,\varphi_{(a,b)}(t)dt \quad (5)$$

Taking the WTr of the signal f(t) as above, and by varying the values of a and b, one can obtain a multi-resolution analysis of the signal of interest. The coefficients corresponding to small values will extract the coarse details of the signal f(t), whereas large values will extract the finer details.

In real-world signals, such as the wind speed signals, the data are discrete. Thus, in practice, the Discrete WTr (DWTr) is used as a wavelet compression method. In DWTr, the values of the factors a and b have discrete values. Hence, the DWTr is computed as:

$$W\,f(m,n) = <\,\varphi_{(m,n)}, f> = \int_{-\infty}^{\infty} f(t)\,\varphi_{(m,n)}\,(t)dt \quad (6)$$

$$\varphi_{(m,n)}\,(t) = 2^{-\frac{m}{2}}\,\varphi\left(\frac{t-n2^m}{2^m}\right) \quad (7)$$

$$\alpha = W^T f \quad (8)$$

where m and n are integers. In DWTr, the wavelet coefficients, a, can be computed numerically. Useful metrics to assess the efficacy of the wavelet compression consist of the total number of the coefficients required to reconstruct the signal, the compression ratio (9), the energy recovery (10), and the mean squared error.

$$Compression\ ratio\ (\%) = \left(1 - \frac{No.of\ C}{No.of\ X}\right) * 100 \quad (9)$$

$$Energy\ recovery\ (\%) = \frac{|XC|^2}{|X|^2} * 100 \quad (10)$$

where X is the vector of wind speed inputs, and C is the vector of the wavelet coefficients to be stored in order to reconstruct the wind speed profile. A high value of energy recovery means that more details of the original signal are restored, and the wind spectrum reconstruction is more accurate.

In practice, the multi-resolution DWTr coefficients are computed by using a series of filtering and sub-sampling operations. For brevity, these details are omitted and can be found in [15]. The distribution of values for the wavelet coefficients is usually centered around 0, with a few large coefficients. This means that almost all the information is concentrated in a small fraction of the coefficients, thus, it can be efficiently compressed. In the following analysis, the Biorthogonal Wavelet 4.4 is chosen as the mother wavelet. The 4.4 indicates the number of vanishing moments for the reconstruction and decomposition filters. It is noted that other wavelets such as the Daubechies wavelet, the Fejer-Korovkin wavelet, the Coiflet wavelet, and the Symlet wavelet were tested and yielded similar results. The results of DWTr on a dataset are a set of high-frequency and low-frequency coefficients. As noted above, the high-frequency coefficients represent the details of the signal, whereas the low-frequency coefficients represent the approximate. The Biorthogonal DWTr is performed on 5 cascading layers. In each layer, the high-frequency coefficients are stored, and the low frequency coefficients are used for the DWTr of the next layer. The workflow of the DWTr is summarized below:

Discrete Wavelet Transform

Step 1. Perform DWTr on the wind speed data using the Biorthogonal Wavelet 4.4 as the mother wavelet to obtain the coefficients from (8).

Step 2. Perform DWTr four more times on the low-frequency coefficients of each layer. Store the coefficients of all layers.

Step 3. Set a threshold to keep only the 10% highest in magnitude coefficients. By doing so, most of the high-frequency coefficients are filtered out, whereas most of the low-frequency coefficients remain.

Step 4. Perform the inverse DWTr (IDWTr) using the remaining wavelet coefficients to obtain the wind speed spectrum.

Table I summarises the results of the wavelet compression on the datasets. In Fig. 3 the wind spectrum reconstructed by the DWTr is plotted together with the real-time spectrum. As it is evident, the reconstructed spectrum closely follows the evolution of the real one. However, several wind fluctuations within seconds are not captured by the DWTr. With more refined thresholding, these fluctuations may be captured more accurately, at the expense of more wavelet coefficients stored. Therefore, there is a trade-off between having to store more coefficients and accepting this limitation.

Table I. DWTr compression results on the wind data sets.

	Low wind speeds	Medium wind speeds
Coefficients stored	63	63
Compression ratio (%)	89.29	89.29
Energy recovery (%)	99.58	99.42
Mean squared error	1.02	0.15

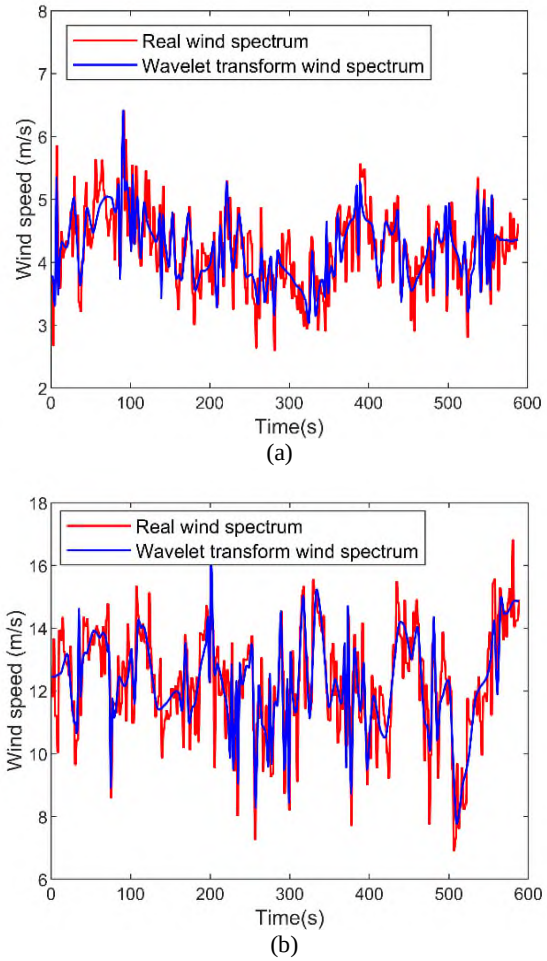

Fig. 3. Comparison of the DWTr wind spectrum with the real wind spectrum for (a) low winds, (b) medium winds.

IV. Electrothermal Modelling and Lifetime Estimation

The effectiveness of employing the reconstructed wind speed profiles to evaluate the turbine converter electrothermal behaviour will be examined in this section. An electrothermal model of a 600kW DD converter is established to calculate the junction temperature profiles of the IGBT and diode by using the reconstructed and original wind speed profiles. Their corresponding damages accumulated during the 10-min periods are then compared to validate that the data reconstructions provided similar lifetime estimations as the real wind speeds.

A. Electrothermal modelling

The electrothermal behaviour of the IGBTs and diodes in a half-bridge power module (Infineon FF1000R17IE4, 1700V/1000A) widely used in the wind industry is assessed by means of an electrothermal simulation model embedded in a 600kW DD turbine model which responds to the change of the wind speed. Four types of wind speed inputs are applied to the model for comparison: 1) high-resolution, real-time wind speeds at 1-sec intervals, 2) real-time 10-min average wind speeds, 3) a reconstruction of the wind spectrum using the RWMH algorithm, 4) a reconstruction of the wind spectrum using the DWTr method.

The model is triggered by the wind speed input, and the shaft speed and the generator RMS current are obtained based on a look-up-table (LUT) of the turbine's characteristics. Subsequently, the junction temperature variation and the power losses of the IGBT and diode are calculated by means of a Cauer network merged with a heatsink model at 25 °C ambient temperature. The thermal network parameters and electrical characteristics of the devices are extracted from the product's datasheet to establish an electrothermal coupling loop for junction temperature calculation [16].

The electrothermal model tracks the wind speed change and reaches the rated 600kW power generation at 12m/s nominal wind speed. Above 12m/s, the generated power is capped at 600kW through turbine pitching. During the modelling process, the generator current cycles of fundamental frequencies are taken into consideration since they can also send the fully rated machine side power converter into deep temperature cycling. Since the converter operates following the variable wind speeds, the current on the devices is a sinewave which has the same RMS value as that of the generator RMS current and the same frequency as that of the wind speed. Thus, the lifetime consumption of the semiconductor devices under low frequency current cycles in a DD turbine system is considered.

B. Lifetime estimation

During thermal cycling, the number of cycles to failure is estimated based on the mean of the junction temperature, T_m, and the amplitude of temperature variation ΔT. The LESIT model [17] indicates a power law dependency for ΔT and an Arrhenius activation energy term for the mean temperature T_m:

$$N_f = A\,\Delta T^{\alpha}\, exp\left(\frac{Q}{R\,T_m}\right) \tag{11}$$

where $A = 640$ and $a = -5$, based on experimental lifetime test results on the devices used in the project. $Q = 7.8\,10^4 J\,mol^{-1}$ and $R = 8.314\,J\,mol^{-1}K^{-1}$ is the gas constant. These depend on the design of the power module, but the values quoted from the previous study are used for comparative evaluation in the present study.

The method used to count the junction temperature cycles is Rainflow Counting (RF) [18]. It breaks down the time-sequence of the junction temperatures into a series of peaks and troughs to count the number of cycles of each $T_m/\Delta T$ case that the device undergoes. The RF method should be used with caution since it does not relate to specific failure rates nor failure mechanisms. Taking that in consideration, it is used to make assessments on the linear damage accumulation, C,on the power devices, in conjunction with the Miner's rule, (12):

$$C = \sum_{i,j} \frac{N_{i,j}}{(N_f)_{i,k}} \tag{12}$$

where $N_{i,j}$ is the number of the cycles observed for the combination of the *i-th* temperature mean and the *j-th* temperature range, and $(N_f)_{i,k}$ is the number of cycles of

fatigue to failure for this combination of mean and range according to (11). When C≅1, failure occurs.

C. Results

The simulation results are illustrated in Figs. 4-7. The first 50 seconds of the simulation are omitted from the graphs, as they represent the transient temperature.

The "Average wind speed" refers to the SCADA 10-min measurements, where the wind speed for the 10-min period is assumed constant and equal to its average value; which is a metric used in traditional reliability assessment methods. In this case, the device temperature varies only due to the current's fundamental cycles. Temperature differences from 1 to 5 degree Celsius are observed, with the diodes more affected. For the low average winds, the temperature variation of both devices shows slight changes around 60 and 300 seconds. This is a result of the low frequency of the current's fundamental cycles which has a larger effect for lower frequencies. Similar behaviour is present in the medium wind speed temperature profiles. However, since the frequency of the current's fundamental cycles is higher, the effect is less evident.

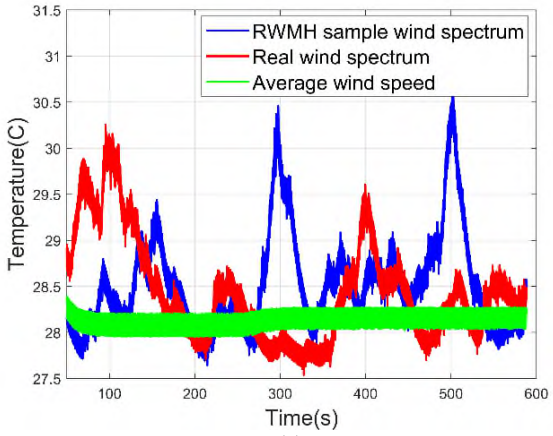

(a)

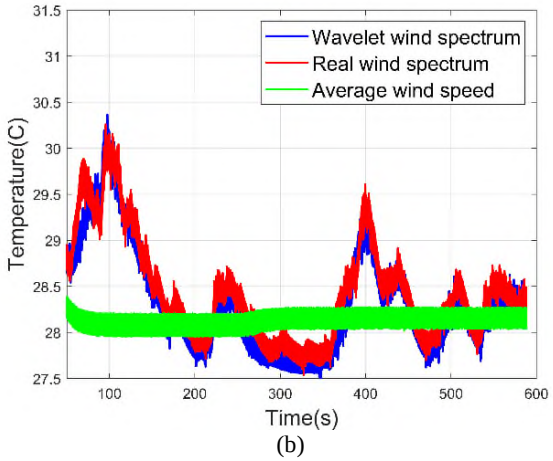

(b)

Fig. 4. Low wind speeds: IGBT temperature variation comparison between real, average, and (a) RWMH sample wind spectrum. (b) DWTr wind spectrum.

As depicted in Figs. 4-7, the temperature varies significantly throughout a 10-min period, as a result of the variable speed operation. It is evident that when the wind speed data are not sampled frequently, important information on the device temperature is lost within the 10-min timeframe. The temperature variation of the RWMH sample wind spectrum demonstrates similar metrics and turbulence features as that of the real wind speeds, even though the spectrum is randomly generated. The DWTr spectrum also shows nearly identical temperature behaviour for both devices, in both instances. As mentioned above, some turbulence features are missed during the wavelet reconstruction, thus explaining some differences in the temperature profiles. Therefore, the electrothermal behaviour can be described effectively and the wind turbulence effect on the lifetime of the devices can be assessed using both methods. A distinct difference between the two methods is that the DWTr addresses the task of wind spectrum reconstruction from a data perspective, building the spectrum according to how it evolved in real-time, but missing some information for better compression ratio. On the other hand, the RWMH addresses the same task from a more physics-based perspective, taking advantage the Gaussian behaviour of the wind in the 10-min timeframe. Thus, it is a method that attempts to emulate the wind's behaviour as a natural phenomenon, using only basic statistical metrics of the 10-min timeframe. Another difference between the methods is that the DWTr requires additional data to be stored, whereas the RWMH algorithm utilizes data already present in the SCADA measurements.

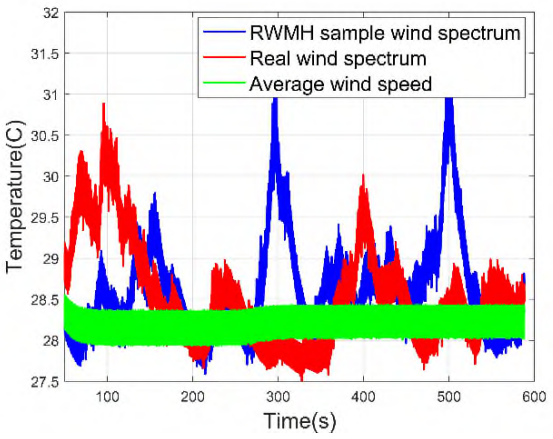

(a)

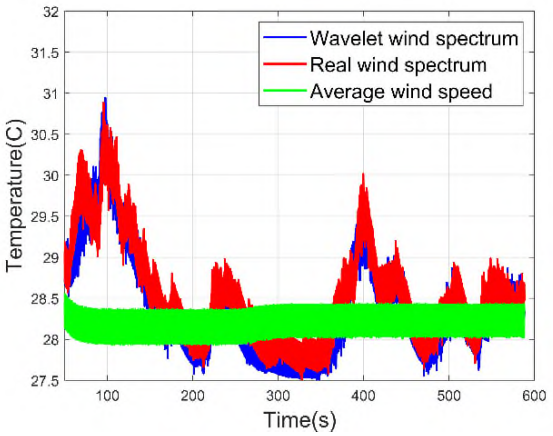

(b)

Fig. 5. Low wind speeds: Diode temperature variation comparison between real, average, and (a) RWMH sample wind spectrum. (b) DWTr wind spectrum.

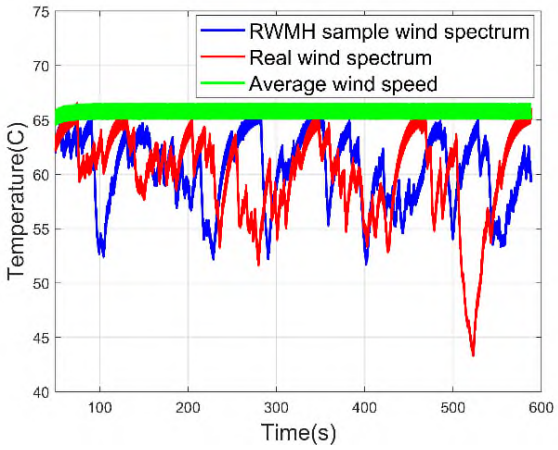

(a)

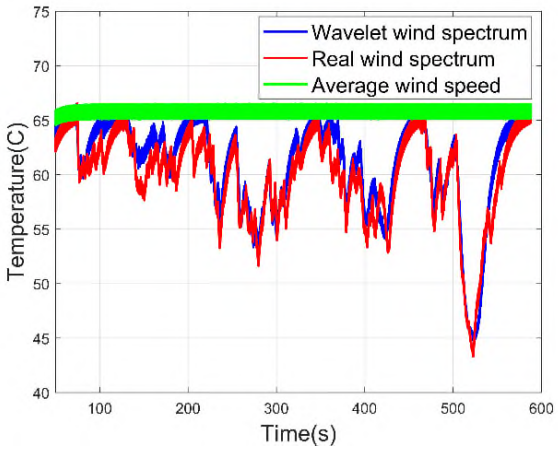

(b)

Fig. 6. Medium wind speeds: IGBT temperature variation comparison between real, average, and (a) RWMH sample wind spectrum. (b) DWTr wind spectrum.

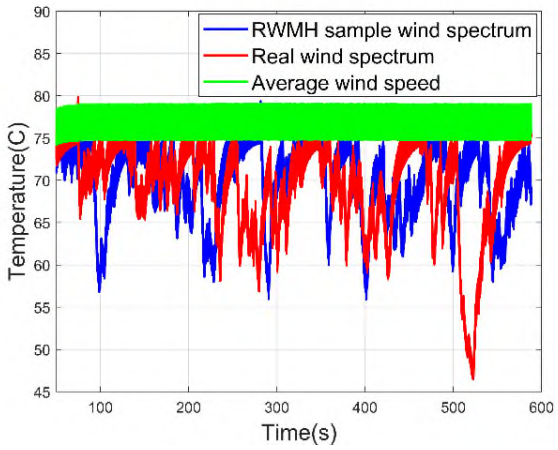

(a)

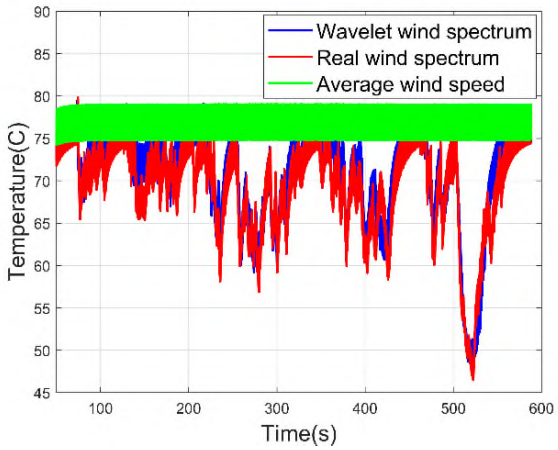

(b)

Fig. 7. Medium wind speeds: Diode temperature variation comparison between real, average, and (a) RWMH sample wind spectrum. (b) DWTr wind spectrum.

The fatigue estimation results show that when the wind speed is not frequently sampled, the damage can be underestimated significantly. Based on the results from Table II, there is a 4 to 7 orders of magnitude difference in damage accumulation between the real temperature profiles of the power devices and their temperature profiles when the wind speed is considered constant for same period, with the average wind speeds predicting less fatigue. Both the RWMH algorithm and the DWTr method yielded results within the same order of magnitude for both devices, in both instances, implying a good accuracy for wind spectrum reconstruction for reliability analysis. The DWTr method's accuracy for reliability estimations is subject to its inability to capture some sudden fluctuations of the wind, occurring within seconds. The RWMH algorithm's accuracy is subject to its stochasticity. In individual 10-min periods the estimated fatigue by the RWMH can deviate from the real fatigue because the spectrum is generated randomly. However, since the wind has a Gaussian behaviour in the 10-min timeframe, these differences cannot be unreasonably large, and will probably be within the same order of magnitude. It is hypothesised that when the algorithm is used to reconstruct the spectrum for longer timeframes, these individual differences will be counteracted by the large number of 10-min operational cycles.

Table II. Reliability assessment results for the 10-min periods.

	Low wind speeds		**Medium wind speeds**	
	C_{IGBT}	C_{Diode}	C_{IGBT}	C_{Diode}
Real spectrum	$2.66\ 10^{-15}$	$6.95\ 10^{-15}$	$2.22\ 10^{-9}$	$2.79\ 10^{-8}$
RWMH spectrum	$7.43\ 10^{-15}$	$1.66\ 10^{-15}$	$1.14\ 10^{-9}$	$1.73\ 10^{-8}$
DWTr spectrum	$3.64\ 10^{-15}$	$8.63\ 10^{-15}$	$1.57\ 10^{-9}$	$1.61\ 10^{-8}$
Average wind speeds	$3.34\ 10^{-20}$	$2.47\ 10^{-19}$	$9.79\ 10^{-16}$	$8.54\ 10^{-13}$

V. Conclusions

This study focuses on the DT concept for reliability assessment of WT power modules. First, a DT framework to examine the electrothermal behaviour of the power modules is proposed. Unlike the traditional reliability assessment methods which utilize SCADA measurements with 10-min sampling frequency, DTs allow for real-time data transfer between the physical power converters and the simulation models embedded in the DT's interface. The importance of integrating the power conversion system with DTs is highlighted by examining the wind turbulence effect on the electrothermal behaviour and the lifetime of the machine side power converters and semiconductor devices in a DD WT. When the fluctuations of the wind that occur within tens of seconds are disregarded by averaging in SCADA, the fatigue experienced by the semiconductors can be significantly underestimated. Based on the simulation results for two 10-

min instances, average wind speeds predict 4 to 7 orders of magnitude lower fatigue experienced by the semiconductor devices. Differences of this magnitude can affect the remaining lifetime estimation of the devices for longer timeframes such as several months or years. Similar behaviour expanded in longer operational cycles may be a reason behind the shorter realistic lifetime of the devices compared to the design's expectations.

To address the issue of the large volume of data required to be stored in DTs, one stochastic method (RWMH algorithm) and one data compression method (DWTr) are proposed to compress the wind data and reconstruct the wind spectrum. These methods may be integrated in the DT services, which is one dimension of the 5-D DT where functions and computations can be executed. Although the RWMH algorithm attempts to reconstruct the wind spectrum randomly, all the turbulence features are captured. The electrothermal behaviour has similar metrics with the real case, and the fatigue prediction is within the same order of magnitude. The DWTr method reconstructs the wind spectrum from a data perspective. Even though it misses some turbulence features, the spectrum generated by DWTr closely resembles the observed. Thus, the temperature profiles of the semiconductor devices are nearly identical to the real profiles. Furthermore, the fatigue predicted by the DWTr is within the same order of magnitude of the real case. Therefore, both methods indicate a promising potential for the task of wind data compression and wind spectrum reconstruction in DT environments.

ACKNOWLEDGMENT

The authors would like to thank Offshore Renewable Energy Catapult for providing useful data to complete this study.

REFERENCES

[1] B. Hahn, M. Durstewitz, and K. Rohrig, "Reliability of Wind Turbines: Experiences of 15 years with 1,500 WTs," *Wind Energy Proc. Euromech Colloq.*, no. July, pp. 329–332, 2007.

[2] F. Spinato, P. J. Tavner, G. J. W. Van Bussel, and E. Koutoulakos, "Reliability of wind turbine subassemblies," *IET Renew. Power Gener.*, vol. 3, no. 4, pp. 387–401, 2009.

[3] S. Yang, D. Xiang, A. Bryant, P. Mawby, L. Ran, and P. Tavner, "Condition monitoring for device reliability in power electronic converters: A review," *IEEE Trans. Power Electron.*, vol. 25, no. 11, pp. 2734–2752, 2010.

[4] I. Van der Hoven, "POWER SPECTRUM OF HORIZONTAL WIND SPEED IN THE FREQUENCY RANGE FROM 0.0007 TO 900 CYCLES PER HOUR," American Meteorological Society, Apr. 2020.

[5] K. Ma, M. Liserre, F. Blaabjerg, and T. Kerekes, "Thermal loading and lifetime estimation for power device considering mission profiles in wind power converter," *IEEE Trans. Power Electron.*, vol. 30, no. 2, pp. 590–602, 2015.

[6] M. Dr. Grieves, "Digital Twin : Manufacturing Excellence through Virtual Factory Replication This paper introduces the concept of a A Whitepaper by Dr . Michael Grieves," *White Pap.*, no. March, 2015.

[7] F. Tao, M. Zhang, and A. Y. C. Nee, "Five-Dimension Digital Twin Modeling and Its Key Technologies," *Digit. Twin Driven Smart Manuf.*, pp. 63–81, 2019.

[8] A. Stetco *et al.*, "Machine learning methods for wind turbine condition monitoring: A review," *Renew. Energy*, vol. 133, pp. 620–635, 2019.

[9] F. Tao, M. Zhang, Y. Liu, and A. Y. C. Nee, "Digital twin driven prognostics and health management for complex equipment," *CIRP Ann.*, vol. 67, no. 1, pp. 169–172, 2018.

[10] Y. Peng, S. Zhao, and H. Wang, "A Digital Twin Based Estimation Method for Health Indicators of DC-DC Converters," *IEEE Trans. Power Electron.*, vol. 36, no. 2, pp. 2105–2118, 2021.

[11] T. Burton, N. Jenkins, D. Sharpe, and E. Bossanyi, *Wind Energy Handbook, Second Edition*. John Wiley and Sons, 2011.

[12] S. Särkkä and A. Solin, "Applied stochastic differential equations," *Appl. Stoch. Differ. Equations*, pp. 1–316, 2019.

[13] S. Brooks, A. Gelman, G. L. Jones, and X. L. Meng, *Handbook of Markov Chain Monte Carlo*. CRC Press, 2011.

[14] S. Mallat, *A Wavelet Tour of Signal Processing*. Elsevier Inc., 2009.

[15] S. G. Mallat, "A Theory for Multiresolution Signal Decomposition: The Wavelet Representation," *IEEE Trans. Pattern Anal. Mach. Intell.*, vol. 11, no. 7, pp. 674–693, 1989.

[16] A. S. Bahman, K. Ma, and F. Blaabjerg, "A Lumped Thermal Model Including Thermal Coupling and Thermal Boundary Conditions for High-Power IGBT Modules," *IEEE Trans. Power Electron.*, vol. 33, no. 3, pp. 2518–2530, Mar. 2018.

[17] M. Held, P. Jacob, G. Nicoletti, P. Scacco, and M. H. Poech, "Fast power cycling test for insulated gate bipolar transistor modules in traction application," *Int. J. Electron.*, vol. 86, no. 10, pp. 1193–1204, 1999.

[18] L. R. GopiReddy, L. M. Tolbert, B. Ozpineci, and J. O. P. Pinto, "Rainflow Algorithm-Based Lifetime Estimation of Power Semiconductors in Utility Applications," *IEEE Trans. Ind. Appl.*, vol. 51, no. 4, pp. 3368–3375, 2015.